ACS chemical biology

Letters

pubs.acs.org/acschemicalbiology

Diacylglycerol Metabolism and Signaling Is a Driving Force Underlying FASN Inhibitor Sensitivity in Cancer Cells

Daniel I. Benjamin,*[,†] Daniel S. Li,[†] Wallace Lowe,[†] Timothy Heuer,[‡] George Kemble,[‡] and Daniel K. Nomura*[,†]

[†]Program in Metabolic Biology, Department of Nutritional Sciences and Toxicology, University of California, Berkeley, Berkeley, California 94720, United States

[‡]3V Biosciences, Inc., 1050 Hamilton Ct., Menlo Park, California 94025, United States

Supporting Information

ABSTRACT: Fatty acid synthase (FASN) generates the *de novo* source of lipids for cell proliferation and is a promising cancer therapy target. Development of FASN inhibitors, however, necessitates a better understanding of sensitive and resistant cancer types to optimize patient treatment. Indeed, testing the cytotoxic effects of FASN inhibition across human cancer cells revealed diverse sensitivities. We show here that metabolic incorporation of glucose into specific complex lipid species strongly predicts FASN inhibitor sensitivity. We also show that the levels of one of these lipid classes, protein kinase C (PKC) stimulator diacylglycerols, are lowered upon FASN inhibitor treatment in sensitive compared to resistant cells and that PKC activators and inhibitors rescue cell death in sensitive cells and sensitize resistant cells, respectively. Our findings not only reveal a biomarker for predicting FASN sensitivity in cancer cells but also a put forth a heretofore unrecognized mechanism underlying the anticancer effects of FASN inhibitors.

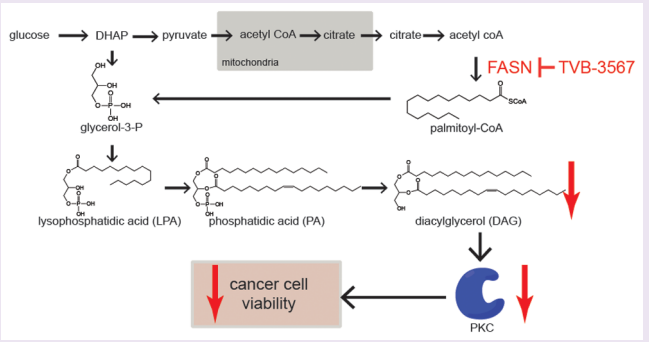

Cancer cells exhibit fundamental metabolic alterations that drive their pathogenic features. Heightened *de novo* lipogenesis, especially through the upregulation of the key lipogenic enzyme fatty acid synthase (FASN) that catalyzes the terminal steps in *de novo* synthesis of fatty acids, is one such major hallmark of cancer cells that is also correlated with poor prognosis in cancer patients.[1] FASN has been shown by many studies to fuel cancer cell proliferation and malignant progression through generating fatty acid precursors required for cell proliferation and energetics, altering membrane fluidity to confer chemotherapy resistance, altering membrane and lipid raft composition to affect tumor-promoting signal transduction and gene expression, regulating the formation of structures that drive invasion such as invadopodia, and generating lipid signaling molecules that fuel oncogenic signaling pathways.[1,2] Given the importance of FASN in various aspects of cancer cell proliferation and progression, pharmacological inhibition of this enzyme has become an increasingly attractive therapeutic strategy to combat cancer. Indeed, since the development of early generation nonselective, irreversible, or cell-impenetrant FASN inhibitors, many pharmaceutical companies have been developing novel, selective, reversible, and *in vivo* effective FASN inhibitors for cancer therapy.[3,4]

While FASN inhibitors are now starting to enter clinical trials, the cancer types that will be sensitive or resistant to FASN inhibitors and whether such sensitivity can be predicted and mechanistically understood is yet unclear. Here, we show that different cancer cell types show vastly different sensitivities to FASN inhibitors and that this sensitivity can be accurately predicted by measuring relative fractional isotopic glucose labeling into specific complex lipid species. We further demonstrate, using metabolomics profiling, that this relative sensitivity or resistance to FASN inhibitors is driven by diacylglycerol (DAG) metabolism and DAG-protein kinase C (PKC) signaling.

RESULTS AND DISCUSSION

FASN Inhibitor Shows Vastly Differing Sensitivities in Impairing Cell Viability Across a Panel of Human Cancer Cells. While blocking FASN is a promising therapeutic strategy for treating cancer, the mechanisms underlying potential sensitivity or resistance to FASN inhibitors remains poorly understood. Here, we have used TVB-3567, a FASN inhibitor developed by 3V Biosciences that is an analog of recently reported imidazopyridine-based molecules,[3] to test the relative effects of FASN inhibition on impairing cellular viability across six different human cancer cells—231MFP and MCF7 breast, C8161 and MUM2C melanoma, PC3 prostate, and SKOV3 ovarian cancer cells. We show that TVB-3567 completely inhibits *de novo* palmitate synthesis *in situ* (1 μM), as measured

Received: February 5, 2015
Accepted: April 14, 2015

DOI: 10.1021/acschembio.5b00240
ACS Chem. Biol. XXXX, XXX, XXX−XXX

by [U−^{13}C]glucose incorporation into fully labeled [^{13}C]-palmitic acid ([^{13}C]C16:0 free fatty acid (FFA)) (m+16), using targeted single-reaction monitoring (SRM)-based liquid chromatography-tandem mass spectrometry (LC-MS/MS) analysis (Figure S1A,B). Interestingly, TVB-3567 showed vastly different sensitivities across these six cell lines, showing the greatest impairments in cell viability in 231MFP, followed by C8161 and MUM2C, with only a modest effect in MCF7, and no effect in PC3 and SKOV3 cells (Figure 1A). We show that

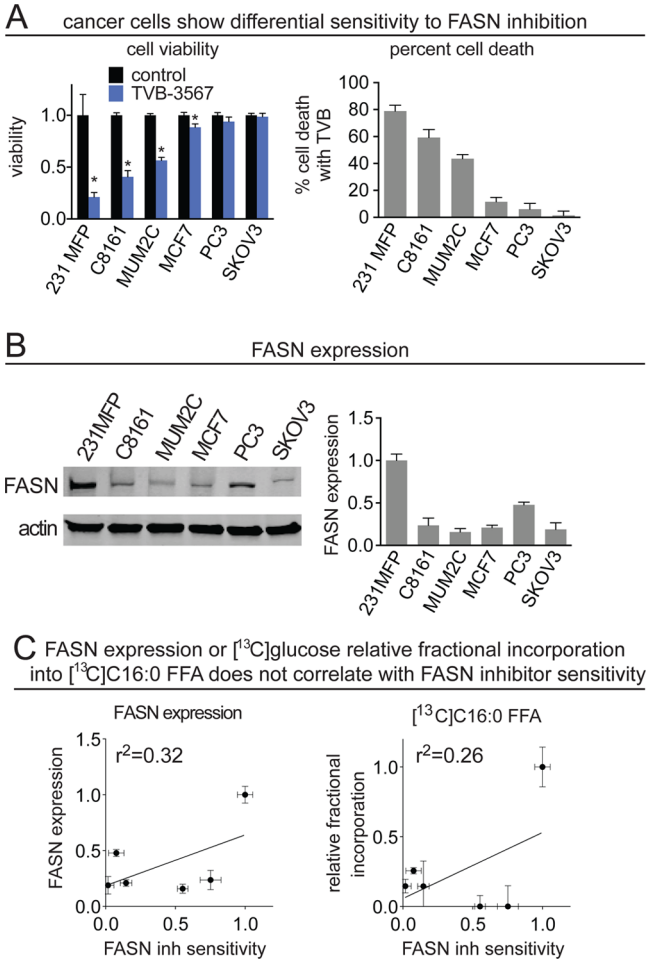

Figure 1. Cancer cells showing differential sensitivity to FASN inhibitor TVB-3567. (A) Cancer cell viability in response to treatment with vehicle DMSO or FASN inhibitor TVB-3567 (1 μM) was measured across a panel of human cancer cells (231 MFP and MCF7 breast cancer, C8161 and MUM2C melanoma, PC3 prostate cancer, and SKOV3 ovarian cancer). Cells were treated with either vehicle DMSO or TVB3567 in 1% serum-containing media, and viability was measured 7 days after treatment by either WST-1 assay or Hoescht staining cell viability assays. (B) FASN expression across the six cancer cell lines, determined by Western blotting and quantified by densitometry across. (C) Cancer cell sensitivity to TVB-3567 is poorly correlated with FASN expression (Pearson correlation coefficient of r^2 = 0.32) and with relative fractional [^{13}C] glucose incorporation into palmitate over 24 h (Pearson correlation coefficient of r^2 = 0.26). For FASN inhibitor sensitivity in C, we have taken the percent cell death data from A and normalized the data against 231MFP sensitivity (set to 1). Relative fractional incorporation of glucose into palmitate was measured by SRM-based LC-MS/MS. Values are expressed as mean ± sem; n = 3−5 per group. Significance is expressed in A as *p < 0.05 compared to control.

these differences in sensitivity to FASN inhibitors can be recapitulated with a less selective FASN inhibitor C75 as well as with siRNA knockdown of FASN in 231MFP and SKOV3 cells (Figure S2). Perhaps more surprising was the lack of correlation between FASN expression and FASN inhibitor sensitivity (Figure 1B,C). We also observed poor correlation between FASN inhibitor sensitivity and relative fractional glucose-derived *de novo* synthesis of fully labeled palmitate, measured by [U−^{13}C]glucose relative fractional incorporation into fully labeled [^{13}C]C16:0 FFA compared to total C16:0 FFA pools (Figure 1C). Overall, our data reveal that different human cancer cell lines show vastly different sensitivities to FASN inhibition and that this sensitivity does not correlate with FASN expression or *de novo* glucose-derived synthesis of palmitic acid.

FASN Inhibitor Sensitivity Correlates with Fractional Glucose-Derived *de Novo* Synthesis of Specific Complex Lipid Species. We next wanted to identify a predictive biomarker that correlated with FASN inhibitor sensitivity. While relative fractional synthesis of [^{13}C]palmitate did not correlate, we conjectured that perhaps [^{13}C]glucose fractional incorporation into complex lipid species compared to their respective total pools would correlate with FASN inhibitor sensitivity. We thus used SRM-based LC-MS/MS metabolomic profiling to measure isotopic incorporation of [^{13}C]glucose not only into [^{13}C]palmitate but also into other acylglycerophospholipids derived from acylation of glucose-derived [^{13}C]-glycerol-3-phosphate (m+3) with [^{13}C]C16:0 FFA (m+16), including [^{13}C]lysophosphatidic acid (LPA) (m+19), [^{13}C]-phosphatidic acid (PA) (m+19), [^{13}C]diacylglycerol (DAG) (m+19), [^{13}C]phosphatidylcholine (PC) (m+19), lysophosphatidylcholine (LPC) (m+19), phosphatidylethanolamine (PE) (m+19), and phosphatidylserine (PS) (m+19), as well as C16:0 acyl carnitine (AC) (m+16) (Figure 2A). We focused on measuring fully labeled lipid species since the majority of [^{13}C]C16:0 FFA was fully labeled (Figures S1A, S3). We show a representative example with [^{13}C]C16:0/C18:1 DAG of how we derived the isotopic SRM programs (Figure S3). Indeed, we were able to detect differential relative fractional incorporation of [^{13}C]glucose into each complex lipid species across the six cancer cell lines (Figure 2B; Table S1). We found that relative fractional synthesis of fully labeled [^{13}C]C16:0 LPA, [^{13}C]-C16:0/C18:1 DAG, [^{13}C]C16:0/C18:1 PC, and [^{13}C]LPC, but not of the other lipid species, strongly correlated with relative FASN inhibitor sensitivity (r^2 > 0.97; Figure 3), suggesting that measuring fractional full incorporation of [^{13}C]glucose into these four specific complex lipids may provide a promising biomarker for FASN sensitivity in cancer cells.

Metabolomic Profiling of FASN Blockade in Sensitive and Resistant Cells Reveals the Importance of DAG Metabolism and Signaling in Driving FASN Inhibitor Anti-Cancer Effects. We next wanted to understand the mechanisms underlying the sensitivity and resistance of cancer cells to FASN inhibitors. We ruled out differences in target engagement in sensitive versus resistant cells, since we see complete blockade of [^{13}C]glucose-derived *de novo* synthesis of multiple complex lipid species *in situ* in both the most sensitive 231MFP and most resistant SKOV3 cancer cells (Figure S4). We next performed SRM-based LC-MS/MS steady-state lipidomic profiling of 154 lipid species in sensitive 231MFP and resistant SKOV3 cells treated with TVB-3567 to identify significant alterations in lipid levels in 231MFP cells that were not present in SKOV3 cells. Among the 154 total lipid species

DOI: 10.1021/acschembio.5b00240
ACS Chem. Biol. XXXX, XXX, XXX−XXX

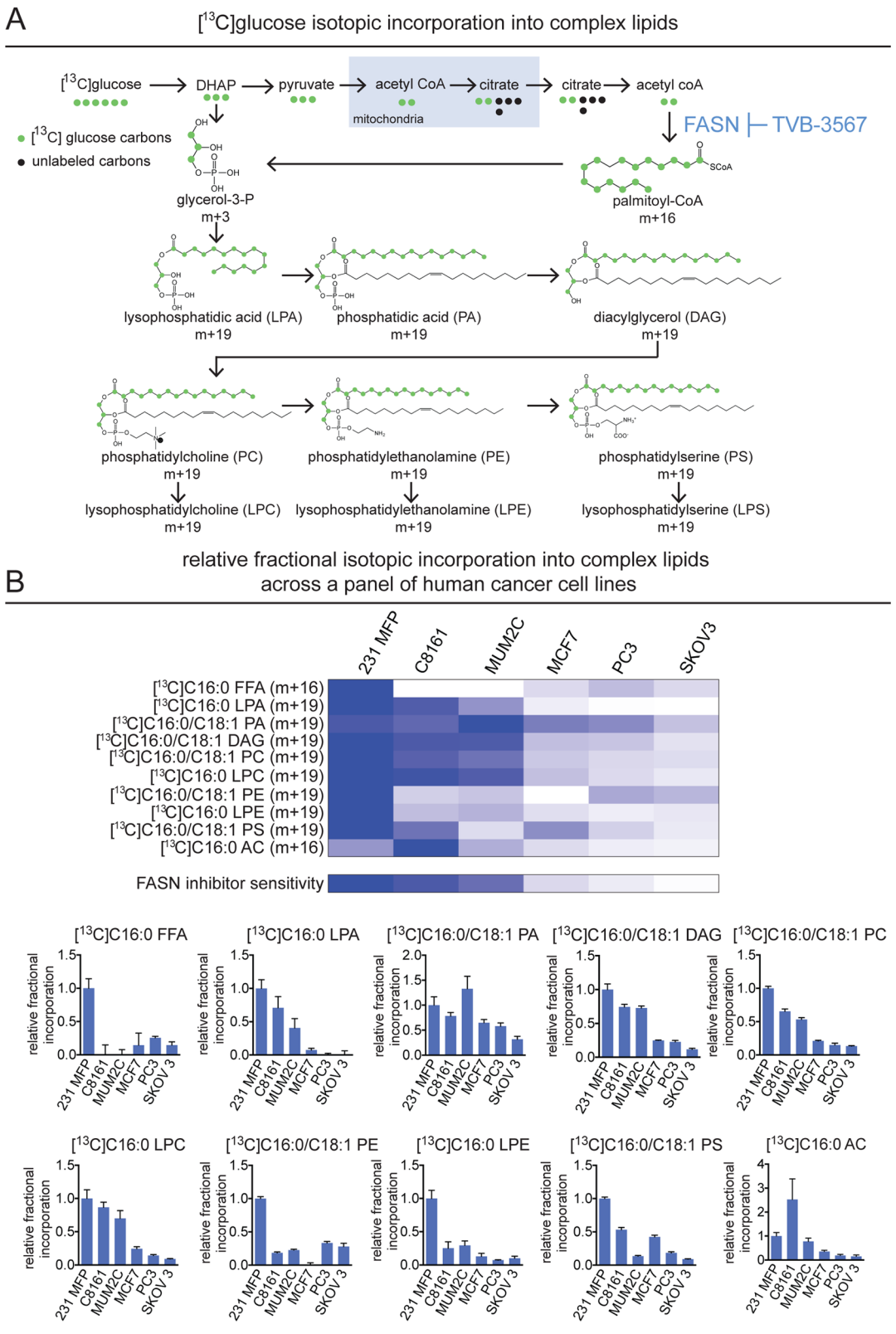

Figure 2. Mapping [^{13}C]glucose relative fractional incorporation into palmitate-containing complex lipid species. (A) Biochemical pathway map describing full [^{13}C]glucose incorporation into complex lipid species through labeling of [^{13}C]glycerol-3-phosphate backbone and [^{13}C]palmitate of complex lipids. (B) Relative fractional [^{13}C]glucose incorporation into fully labeled [^{13}C]palmitate and palmitate containing complex lipid species. The relative fractional incorporation of isotopic glucose into each complex lipid species was calculated by dividing the levels of full isotopic incorporation into the particular lipid species in 24 h in the [^{13}C]glucose-treated cells by the steady-state levels of the corresponding [^{12}C]lipid species in the [^{12}C]glucose-treated cells in 24 h and then normalized to the fractional incorporation in 231MFP cells. This relative fractional incorporation is displayed as both a heat map as well as individual bar graphs for each lipid species. Dark and light blue on the heat map denote high and low fractional incorporation, respectively. Data are presented as mean ± sem; n = 4 per group.

DOI: 10.1021/acschembio.5b00240
ACS Chem. Biol. XXXX, XXX, XXX−XXX

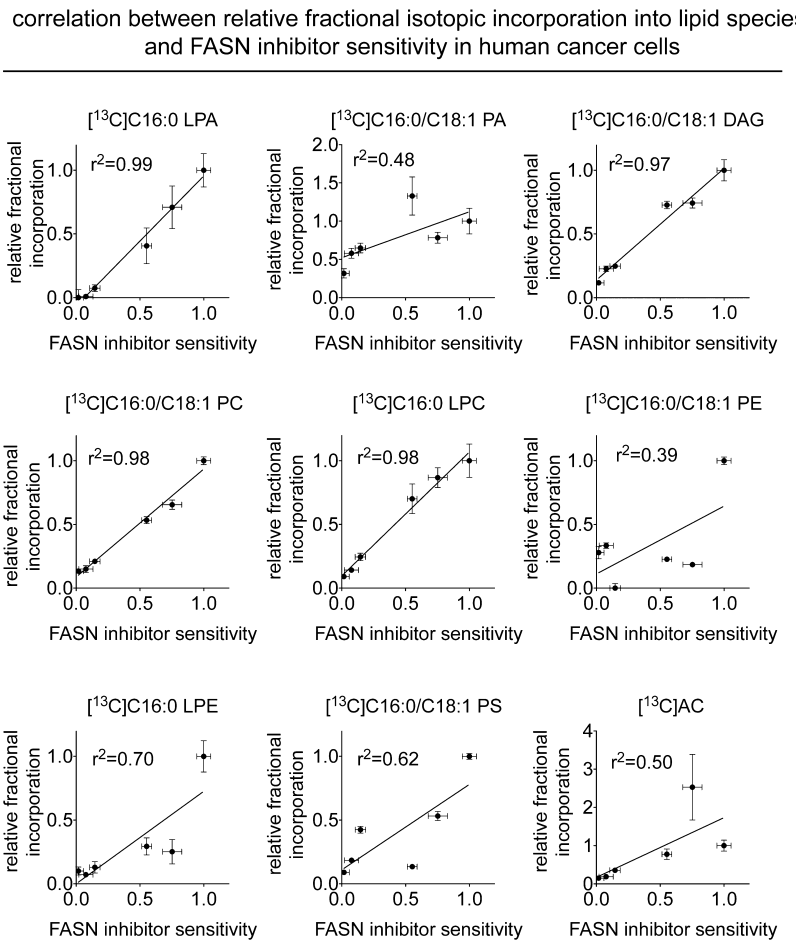

Figure 3. Correlation between relative fractional incorporation of isotopic glucose into complex lipid species and FASN inhibitor sensitivity reveals predictive biomarkers. We show correlation plots between FASN inhibitor sensitivity and fractional isotopic incorporation of [^{13}C]glucose into fully labeled complex lipids. We find that [^{13}C] C16:0 LPA, C16:0/18:1 DAG, C16:0/18:1 PC, and C16:0 LPC (all m+19), but not other lipid species, strongly correlate with TVB-3567 sensitivity across the six cancer cell lines tested in Figure 1 (Pearson correlation coefficients of $r^2 > 0.97$). Data are presented as mean ± sem; $n = 4$ per group.

that were quantified, intriguingly, we found that the only lipid species that showed significant and >3-fold changes upon TVB-3567 treatment in 231MFP cells belonged to the DAG and LPA/LPA-ether (LPAe) family of lipids (Figure 4A; Table S1; Figure S5). Both DAG and LPA were also highly correlated in their relative fractional isotopic incorporation with FASN inhibitor sensitivity (Figure 3). More interestingly, we find that the resistant SKOV3 cells show significantly less or no reduction in the levels of DAGs and LPA/LPAe compared to the sensitive 231MFP cells upon FASN inhibition with both TVB-3567 and C75 treatment, suggesting that these lipid species may play a role in conferring sensitivity and resistance to FASN inhibitors (Figure 4B; Figure S5). We also show that FASN knockdown by RNA interference recapitulates the effects shown with pharmacological blockade of FASN, in which FASN knockdown lowers DAG and LPA/LPAe levels to a higher degree in 231MFP cells compared to SKOV3 cells (Figure S5). Indeed, both DAG and LPA/LPAe lipid classes are known oncogenic signaling lipids that promote cancer pathogenicity through stimulating protein kinase C and LPA receptor signaling pathways, respectively.[5,6] We thus performed rescue experiments with LPA (200 nM) and a PKC agonist phorbol 12-myristate 13-acetate (PMA; 1 μM) and show that PMA, but not LPA, completely rescues the cell viability impairments conferred by TVB-3567 in 231MFP cells (Figure 4C). We also show that the resistant SKOV3 cells become sensitized to FASN inhibition upon treatment with a PKC inhibitor Go 6983 (Figure 4D).

Previous studies have shown that PKC promotes cell survival through phosphorylation of its downstream substrate p90^{RSK}, leading to phosphorylation and inactivation of the pro-apoptotic factor Bad.[7] We show here that FASN inhibition by TVB-3567 impairs the phosphorylation of the p90^{RSK} target, ribosomal protein S6, and that PMA rescues this impairment in sensitive 231MFP cells (Figure 4E). While PKC or FASN inhibition alone does not affect or only modestly lowers phosphorylated S6, we show that dual inhibition of PKC and FASN robustly and significantly lowers phosphorylated S6 levels in the resistant SKOV3 cells (Figure 4F). We note that PKC expression does not correlate with FASN inhibitor sensitivity. Furthermore, the TVB-3567-mediated reductions in DAG levels are not rescued by PKC activation with PMA, and PKC inhibition by Go6983 alone or in conjunction with TVB-3567 also does not alter DAG levels (Figure S6). Taken together, our results show that FASN inhibitor sensitivity is driven by reductions in DAG levels and impairments in DAG-PKC signaling pathways, and that combinatorial inhibition of FASN and PKC synergistically impairs PKC signaling pathways to sensitize FASN inhibitor-resistant cancer cells.

DOI: 10.1021/acschembio.5b00240
ACS Chem. Biol. XXXX, XXX, XXX−XXX

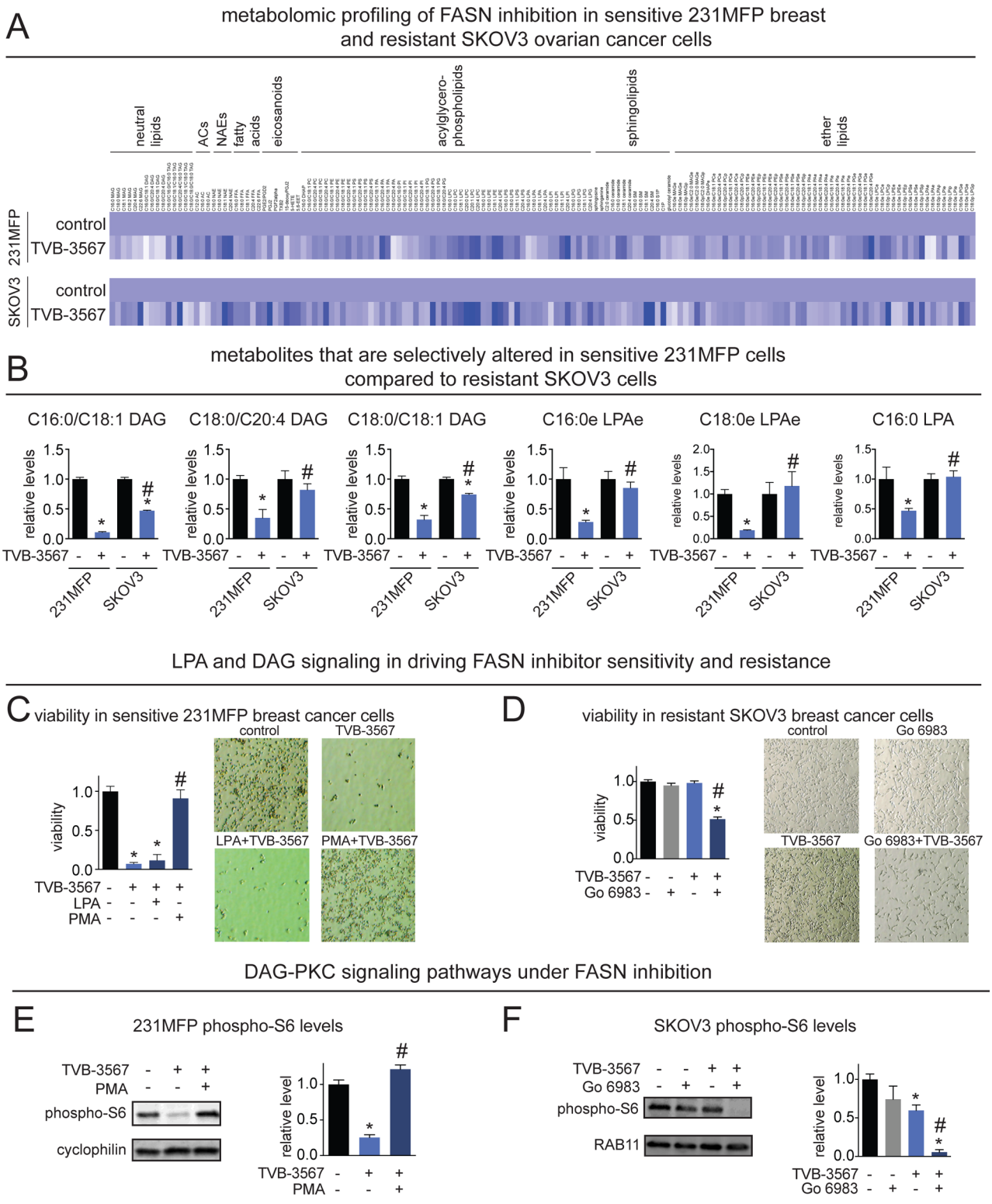

Figure 4. Metabolomic profiling of FASN inhibition revealing diacylglycerol metabolism and signaling as important drivers of FASN inhibitor sensitivity. (A) We performed an SRM-based LC-MS/MS steady-state metabolomic analysis of 154 lipid species to identify metabolomics alterations upon FASN inhibition in the sensitive 231MFP and resistant SKOV3 cells. 231MFP and SKOV3 cells were treated with vehicle (DMSO, 0.1%) or TVB-3567 (1 μM) for 24 h in serum-free media, after which cellular lipidomes were subjected to metabolomic analysis. The heat map shows the relative levels of all lipids measured in this experiment normalized to their respective controls. Darker and lighter blue shading on the heat map corresponds to higher and lower relative metabolite levels compared with DMSO treated controls, respectively. (B) We wanted to identify metabolites that were significantly changing in the sensitive 231MFP cells that were altered less or were not changing in the resistant SKOV3 cells, as these lipid species may represent drivers of FASN inhibitor sensitivity. Shown are the relative levels of metabolites that were significantly ($p < 0.05$) and robustly (>3-fold) altered in 231MFP cells and not in SKOV3 cells compared with respective vehicle-treated controls. Relative levels are normalized to the controls of each respective cell line. FASN inhibition with TVB-3567 significantly and robustly lowers levels of DAGs and LPA/LPA-ether (LPAe) species in 231MFP cells but not in SKOV3 cells. (C) The cell viability impairments conferred by TVB-3567 treatment in

DOI: 10.1021/acschembio.5b00240
ACS Chem. Biol. XXXX, XXX, XXX−XXX

Figure 4. continued

231MFP cells (1 μM) was significantly rescued by the addition of the DAG-independent PKC activator PMA (1 μM) but not by LPA (200 nM). (D) Treatment of SKOV3 cells with the PKC inhibitor Go 6983 (1 μM) hypersensitizes them to FASN inhibition with TVB-3567. Pharmacological agents in C and D were cotreated in 231MFP cells for 4 days in serum-free media, and cell viability was measured using the Hoescht stain cell viability assay. (E, F) Levels of phosphorylated ribosomal protein S6 upon treatment of 231MFP or SKOV3 cells with vehicle (DMSO), TVB-3567 (1 μM), PMA (1 μM), and/or Go 6983 (1 μM) for 3 days in serum-free media. Phospho-S6 was quantified in relation to expression of loading controls cyclophilin and RAB11 for 231MFP and SKOV3, respectively. Data are presented as mean ± sem; n = 4−5 per group. Significance is presented in (B−F) as *p < 0.05 compared with vehicle-treated control and # p < 0.05 between 231 MFP and SKOV3 TVB-3567 treated groups.

Our metabolomic profiling also revealed that the tumor-suppressing signaling lipid ceramide was also elevated upon FASN inhibition in 231MFP cells, but this lipid was significantly lowered in the resistant SKOV3 cells (Figure S7A). Indeed, previous studies have shown that FASN inhibition leads to elevated ceramides causing apoptosis.[1] We show that inhibiting ceramide synthesis leads to reduced ceramide levels and partially rescued cell viability in TVB-3567-treated 231MFP cells (Figure S7B,C).

Taken together, our results reveal that the cytotoxic effects of FASN inhibitors in sensitive lines may be due to the robust depletion of oncogenic signaling lipids, such as DAGs, and the elevation of tumor-suppressing ceramides. We also show that resistance to FASN inhibitors may be overcome by dual PKC and FASN blockade, opening up the possibility for synergistic chemotherapeutic options for FASN inhibitors.

Conclusions. Many studies have shown that FASN is heightened in cancer cells and that FASN blockade impairs cancer pathogenicity and tumorigenesis, making FASN an attractive target for cancer therapy. Multiple mechanisms have been reported for the anticancer effects of FASN inhibitors, including a disruption in lipid rafts that control oncogenic signaling pathways, depletion of lipids required for maintenance of cell membranes, and toxic accumulation of malonyl-CoA leading to accumulation of ceramide and apoptosis.[1] While these mechanisms have explained the broad anticancer effects of many different types of cancer cells to FASN inhibition, a predictive and mechanistic understanding underlying resistance of certain cancer cell types to FASN inhibition has remained enigmatic. Here, we show that different cancer cell types show varying sensitivities to FASN inhibitors and that this sensitivity or resistance can be predicted, not by FASN expression or fractional *de novo* synthesis in the FASN product palmitate, but rather by fractional incorporation of glucose into specific complex lipids, including LPA, DAG, LPC, and PC. We further show that the sensitivity and resistance of FASN inhibitors is driven by differences between cell types in maintaining DAG levels and DAG-PKC signaling in the face of FASN inhibition, and that resistance to FASN inhibitors may be overcome by treatment with both FASN and PKC inhibitors.

While our study reveals a novel mechanism underlying FASN inhibitor sensitivity in cancer cells, we cannot rule out alternative mechanisms of resistance that may play a role in *in vivo* tumorigenesis, including the contributions of exogenous lipids such as palmitate and lysophospholipids.[8,9] Indeed, it will be of future interest to determine the relative contribution of exogenous carbon sources (e.g., glucose, glutamine, fatty acids, lysophospholipids) as well as endogenous lipolytic sources in maintaining membrane, lipid raft, and signaling lipids in cancer cells toward fully understanding the therapeutic potential of manipulating cancer cell lipid metabolism.[8−11] It will also be of future interest to understand whether our findings can be extended *in vivo* in both cancer models and in patients. Taken together, our findings reveal potential biomarkers that may inform patient responsiveness to FASN inhibitors, put forth a novel mechanism underlying FASN inhibitor anticancer effects, and propose a possible route to sensitize FASN inhibitor-resistant tumors.

EXPERIMENTAL PROCEDURES

Materials. MUM2C, MCF7, and PC3 cell lines were purchased from ATCC. C8161 cells were provided by Mary Hendrix. The 231MFP and SKOV3 cells were generated from explanted xenograft tumors of MDA-MB-231 and parental SKOV3 cells, respectively, as described previously.[12] TVB-3567 was obtained from 3-V Biosciences. The structure of TVB-3567 cannot be disclosed at this time due to its proprietary nature. TVB-3567 can be obtained by contacting 3-V Biosciences. TVB-3567, PKC activator PMA (Tocris), and PKC inhibitor Go 6983 (Tocris) were used at 1 μM final concentration, based on discussion with 3-V Biosciences or previously reported studies. LPA (Avanti) was treated at a final concentration of 200 nM. The ceramide synthesis inhibitors fumonsin B1 (Cayman), GW4869 (Cayman), and 1-aminodecylidene bis-phosphonic acid (Cayman) were treated at a final concentration of 10, 2, and 0.5 μM, respectively. siControl and siFASN oligonucleotides were obtained from Dharmacon GE Lifesciences.

Cell Culture Conditions. SKOV3, C8161, MUM2C, and MCF7 cells were cultured in RPMI1640 media containing 10% fetal bovine serum (FBS) and 2 mM glutamine maintained at 37 °C at 5% CO_2. PC3 cells were cultured in F12K media containing 10% FBS and 2 mM glutamine and were maintained at 37 °C at 5% CO_2. 231MFP cells were cultured in L15 media containing 10% FBS and 2 mM glutamine and were maintained at 37 °C in 0% CO_2.

Cell Viability Studies. Cells were washed twice in PBS, harvested by trypsinization, washed in serum-free media, and seeded into 96-well plates (30 000 cells per well in a volume of 200 μL containing 1% FBS) for 0 and 7 days prior to the addition of WST-1 (10 μL) for 1 h at 37 °C in 5% CO_2. Absorbance was then measured at 450 nm using a spectrophotometer. For 231MFP cells, rather than the addition of WST-1, cell viability was measured at 0 and 7 days by first aspirating the media followed by the addition of 100 μL of fixation solution containing 5 μM Hoescht in formalin. The fixation solution was aspirated, and the cells were washed with PBS. Absorbance was then measured using a fluorescent plate reader with an excitation of 350 nm and an emission of 461 nm. For both viability assays, cells were seeded into 6 cm dishes (side-by-side with 96-well plates) for the purpose of imaging.

Metabolomic Profiling of Cancer Cells. Metabolite measurements were conducted using modified previous procedures.[13] Cancer cells were grown in serum-free media for 24 h to minimize the contribution of serum-derived metabolites to the cellular profiles. Cancer cells (1×10^6 cells/6 cm dish or 2×10^6 cells/6 cm dish) were washed twice with phosphate buffer saline (PBS), harvested by scraping, and isolated by centrifugation at 1400g at 4 °C, and cell pellets were flash frozen and stored at −80 °C until metabolome extractions. Lipid metabolites were extracted in 4 mL of a 2:1:1 mixture of chloroform/methanol/Tris buffer with inclusion of internal standards C12:0 dodecylglycerol (10 nmol) and pentadecanoic acid (10 nmol). Organic and aqueous layers were separated by centrifugation at 1000g for 5 min, and the organic layer was collected. The aqueous layer was acidified (for metabolites such as LPA) by

DOI: 10.1021/acschembio.5b00240
ACS Chem. Biol. XXXX, XXX, XXX−XXX

adding 0.1% formic acid, followed by the addition of 2 mL of chloroform. The mixture was vortexed, and the organic layers were combined, dried down under N_2, and dissolved in 120 μL of chloroform, of which 10 μL was analyzed by both single-reaction monitoring (SRM)-based LC-MS/MS or untargeted LC-MS. LC separation was achieved with a Luna reverse-phase C5 column (50 mm × 4.6 mm with 5 μm diameter particles, Phenomenex). Mobile phase A was composed of a 95:5 ratio of water/methanol, and mobile phase B consisted of 2-propanol, methanol, and water in a 60:35:5 ratio. Solvent modifiers 0.1% formic acid with 5 mM ammonium formate and 0.1% ammonium hydroxide were used to assist ion formation as well as to improve the LC resolution in both positive and negative ionization modes, respectively. The flow rate for each run started at 0.1 mL/min for 5 min, to alleviate backpressure associated with injecting chloroform. The gradient started at 0% B and increased linearly to 100% B over the course of 45 min with a flow rate of 0.4 mL/min, followed by an isocratic gradient of 100% B for 17 min at 0.5 mL/min before equilibrating for 8 min at 0% B with a flow rate of 0.5 mL/min.

MS analysis was performed with an electrospray ionization (ESI) source on an Agilent 6430 QQQ LC-MS/MS. The capillary voltage was set to 3.0 kV, and the fragmentor voltage was set to 100 V. The drying gas temperature was 350 °C, the drying gas flow rate was 10 L/min, and the nebulizer pressure was 35 psi. Representative metabolites were quantified by SRM of the transition from precursor to product ions at associated collision energies. Data were normalized to the internal standards, and also external standard curves of metabolite classes against the internal standards and levels were expressed as relative metabolite levels compared to controls. The raw data from these studies are in Table S1. LPA and DAGs were specifically quantified with unnatural internal standards C13:0 LPA and C15:0/C18:1 DAG, respectively. These internal standards were added alongside dodecylglycerol and pentadecanoic acid in the 2:1:1 chloroform/methanol/Tris buffer mixture. These data are in Figure S5C.

Analysis of Isotopic Glucose Incorporation into Lipid Species. Isotopic glucose incorporation into lipids was measured by labeling cells with [^{12}C] or [U−^{13}C] glucose and quantifying both nonisotopic and isotopic incorporation into lipid species. Cells were treated with either 10 mM [^{12}C]glucose or [^{13}C]glucose in otherwise glucose-free RPMI media. Cells were harvested 24 h after labeling with [^{12}C]/[^{13}C]glucose, and the lipid metabolome was extracted as previously described and analyzed by SRM-based targeted LC-MS/MS for both nonisotopic and isotopic lipid species. The relative fractional incorporation of isotopic glucose into each complex lipid species was calculated by dividing the levels of isotopic incorporation into the particular lipid species in 24 h in the [^{13}C]glucose-treated cells by the steady-state levels of the corresponding [^{12}C]lipid species in the [^{12}C]glucose-treated cells in 24 h, and then normalized to the fractional incorporation in 231MFP cells (set to 1).

Western Blotting. Cells were lysed by probe sonication in PBS containing both protease and phosphatase inhibitors. Proteins were resolved by electrophoresis on 4−15% Tris-Glycine precast Mini-PROTEAN TGX gel (BioRad Laboratories) and transferred to PVDF membranes using the iBlot system (Invitrogen). Blots were blocked with 5% nonfat milk in a Tris-buffered saline containing Tween-20 (TBST) solution for 60 min at RT, washed in 1× TBST, and probed with primary antibody of interest diluted in 5% BSA TBST solution. Following three subsequent TBST washes, the blots were incubated in the dark with a IR-linked secondary at RT for 1 h. Following three more washes, blots were visualized using an Odyssey Li-Cor scanner.

■ ASSOCIATED CONTENT

Ⓢ Supporting Information

Seven figures and a table are provided. This material is available free of charge via the Internet at http://pubs.acs.org.

■ AUTHOR INFORMATION

Corresponding Authors

*E-mail: danielbenjamin@berkeley.edu.

*E-mail: dnomura@berkeley.edu.

Author Contributions

D.I.B. designed research, performed research, analyzed data, and wrote the paper. D.K.N. designed research, performed research, analyzed data, and wrote the paper. T.H. and G.K. provided reagents for the study.

Notes

The authors declare the following competing financial interest(s): D.K.N. is a paid consultant, T.H. is a Senior Director, and G.K. is the Chief Scientific Officer of 3-V Biosciences. T.H. and G.K. are paid employees and shareholders of 3-V Biosciences and are developing FASN inhibitors into the clinic. This data in this study was not funded by 3-V Biosciences.

■ ACKNOWLEDGMENTS

We thank the members of the Nomura Research Group for critical reading of the manuscript. This work was supported by grants from the National Institutes of Health (R01CA172667 for D.I.B. and D.K.N.), American Cancer Society Research Scholar Award (RSG14-242-01-TBE for D.I.B., D.K.N.), DOD Breakthroughs Award, and the Searle Scholar Foundation (D.K.N.).

■ REFERENCES

(1) Menendez, J. A., and Lupu, R. (2007) Fatty acid synthase and the lipogenic phenotype in cancer pathogenesis. *Nat. Rev. Cancer 7*, 763−777.

(2) Louie, S. M., Roberts, L. S., and Nomura, D. K. (2013) Mechanisms linking obesity and cancer. *Biochim. Biophys. Acta, Mol. Cell Biol. Lipids 1831*, 1499−1508.

(3) Oslob, J. D., Johnson, R. J., Cai, H., Feng, S. Q., Hu, L., Kosaka, Y., Lai, J., Sivaraja, M., Tep, S., Yang, H., Zaharia, C. A., Evanchik, M. J., and McDowell, R. S. (2013) Imidazopyridine-Based Fatty Acid Synthase Inhibitors That Show Anti-HCV Activity and in Vivo Target Modulation. *ACS Med. Chem. Lett. 4*, 113−117.

(4) Pandey, P. R., Liu, W., Xing, F., Fukuda, K., and Watabe, K. (2012) Anti-cancer drugs targeting fatty acid synthase (FAS). *Recent Pat. Anti-Cancer Drug Discovery 7*, 185−197.

(5) Griner, E. M., and Kazanietz, M. G. (2007) Protein kinase C and other diacylglycerol effectors in cancer. *Nat. Rev. Cancer 7*, 281−294.

(6) Mills, G. B., and Moolenaar, W. H. (2003) The emerging role of lysophosphatidic acid in cancer. *Nat. Rev. Cancer 3*, 582−591.

(7) Tan, Y., Ruan, H., Demeter, M. R., and Comb, M. J. (1999) p90(RSK) blocks bad-mediated cell death via a protein kinase C-dependent pathway. *J. Biol. Chem. 274*, 34859−34867.

(8) Kamphorst, J. J., Cross, J. R., Fan, J., de Stanchina, E., Mathew, R., White, E. P., Thompson, C. B., and Rabinowitz, J. D. (2013) Hypoxic and Ras-transformed cells support growth by scavenging unsaturated fatty acids from lysophospholipids. *Proc. Natl. Acad. Sci. U.S.A. 110*, 8882−8887.

(9) Louie, S. M., Roberts, L. S., Mulvihill, M. M., Luo, K., and Nomura, D. K. (2013) Cancer cells incorporate and remodel exogenous palmitate into structural and oncogenic signaling lipids. *Biochim. Biophys. Acta, Mol. Cell Biol. Lipids 1831*, 1566−1572.

(10) Mullen, A. R., Wheaton, W. W., Jin, E. S., Chen, P. H., Sullivan, L. B., Cheng, T., Yang, Y., Linehan, W. M., Chandel, N. S., and DeBerardinis, R. J. (2012) Reductive carboxylation supports growth in tumour cells with defective mitochondria. *Nature 481*, 385−388.

(11) Nomura, D. K., Long, J. Z., Niessen, S., Hoover, H. S., Ng, S. W., and Cravatt, B. F. (2010) Monoacylglycerol lipase regulates a fatty acid network that promotes cancer pathogenesis. *Cell 140*, 49−61.

DOI: 10.1021/acschembio.5b00240
ACS Chem. Biol. XXXX, XXX, XXX−XXX

(12) Jessani, N., Humphrey, M., McDonald, W. H., Niessen, S., Masuda, K., Gangadharan, B., Yates, J. R., 3rd, Mueller, B. M., and Cravatt, B. F. (2004) Carcinoma and stromal enzyme activity profiles associated with breast tumor growth in vivo. *Proc. Natl. Acad. Sci. U.S.A. 101*, 13756−13761.

(13) Benjamin, D. I., Cozzo, A., Ji, X., Roberts, L. S., Louie, S. M., Mulvihill, M. M., Luo, K., and Nomura, D. K. (2013) Ether lipid generating enzyme AGPS alters the balance of structural and signaling lipids to fuel cancer pathogenicity. *Proc. Natl. Acad. Sci. U.S.A. 110*, 14912−14917.

DOI: 10.1021/acschembio.5b00240
ACS Chem. Biol. XXXX, XXX, XXX−XXX